Tunable lasing on silver island films by coupling to the localized surface plasmon

Shuya Ning, Zhaoxin Wu,* Hua Dong, Fang Yuan, Lin Ma, Bo Jiao, and Xun Hou

Key Laboratory of Photonics Technology for Information, Department of Electronic Science and technology, School of Electronic and Information Engineering, Xi'an Jiaotong University, Xi'an, 710049, China
**zhaoxinwu@mail.xjtu.edu.cn*

Abstract: Lasing of N,N'-bis(3-methylphenyl)-N,N'-diphenyl-[1,1':4',1"-terphenyl]-4,4"-diamine (BMT-TPD) films on silver island films (SIFs) was investigated. The size of silver nanoparticles (NPs) of SIFs ranged from 8 to 500 nm, which showed the different localized surface plasmon resonance (LSPR). It was found that the lasing wavelength of BMT-TPD was tuned by the LSPR peaks of silver NPs. This was attributed to the coupling between gain medium and plasmonic silver NPs, that is, the surface plasmon amplification by stimulated emission of radiation which resulted in the lasing at the corresponding wavelengths. This is expected to be a new and easy approach for the tuning of wavelength of lasing.

OCIS codes: (140.0140) Lasers and laser optics; (140.2050) Dye lasers; (140.3600) Lasers, tunable; (250.5403) Plasmonics.

References and links

1. D. J. Bergman and M. I. Stockman, "Surface plasmon amplification by stimulated emission of radiation: quantum generation of coherent surface plasmons in nanosystems," Phys. Rev. Lett. **90**(2), 027402 (2003).
2. M. I. Stockman, "Spasers explained," Nat. Photonics **2**(6), 327–329 (2008).
3. R. F. Oulton, V. J. Sorger, T. Zentgraf, R. M. Ma, C. Gladden, L. Dai, G. Bartal, and X. Zhang, "Plasmon lasers at deep subwavelength scale," Nature **461**(7264), 629–632 (2009).
4. M. A. Noginov, G. Zhu, A. M. Belgrave, R. Bakker, V. M. Shalaev, E. E. Narimanov, S. Stout, E. Herz, T. Suteewong, and U. Wiesner, "Demonstration of a spaser-based nanolaser," Nature **460**(7259), 1110–1112 (2009).
5. H. A. Atwater and A. Polman, "Plasmonics for improved photovoltaic devices," Nat. Mater. **9**(3), 205–213 (2010).
6. L. Dong, F. Ye, A. Chughtai, S. Popov, A. T. Friberg, and M. Muhammed, "Photostability of lasing process from water solution of Rhodamine 6G with gold nanoparticles," Opt. Lett. **37**(1), 34–36 (2012).
7. M. I. Stockman, "The spaser as a nanoscale quantum generator and ultrafast amplifier," J. Opt. **12**(2), 024004 (2010).
8. V. M. Parfenyev and S. S. Vergeles, "Intensity-dependent frequency shift in surface plasmon amplification by stimulated emission of radiation," Phys. Rev. A **86**(4), 043824 (2012).
9. D. J. Bergman and M. I. Stockman, "Surface Plasmon Amplification by Stimulated Emission of Radiation: Quantum Generation of Coherent Surface Plasmons in Nanosystems," Phys. Rev. Lett. **90**(2), 027402 (2003).
10. P. Anger, P. Bharadwaj, and L. Novotny, "Enhancement and quenching of single-molecule fluorescence," Phys. Rev. Lett. **96**(11), 113002 (2006).
11. T. H. Taminiau, F. D. Stefani, F. B. Segerink, and N. F. van Hulst, "Optical antennas direct single-molecule emission," Nat. Photonics **2**(4), 234–237 (2008).
12. A. Kinkhabwala, Z. Yu, S. Fan, Y. Avlasevich, K. Müllen, and W. E. Moerner, "Large single-molecule fluorescence enhancements produced by a bowtie nanoantenna," Nat. Photonics **3**(11), 654–657 (2009).
13. G. Baffou, C. Girard, E. Dujardin, G. Colas des Francs, and O. Martin, "Molecular quenching and relaxation in a plasmonic tunable system," Phys. Rev. B **77**(12), 121101 (2008).
14. P. Mühlschlegel, H. J. Eisler, O. J. F. Martin, B. Hecht, and D. W. Pohl, "Resonant optical antennas," Science **308**(5728), 1607–1609 (2005).
15. M. Fukushima, H. Yanagi, and Y. Taniguchi, "Distributed feedback lasing from dye-doped glass films using photopatterned gold nanoparticles," J. Appl. Phys. **97**(10), 106104 (2005).
16. J. Stehr, J. Crewett, F. Schindler, R. Sperling, G. von Plessen, U. Lemmer, J. M. Lupton, T. A. Klar, J. Feldmann, A. W. Holleitner, M. Forster, and U. Scherf, "A low threshold polymer laser based on metallic nanoparticle gratings," Adv. Mater. **15**(20), 1726–1729 (2003).

#230988 - $15.00 USD Received 22 Dec 2014; revised 8 Feb 2015; accepted 8 Feb 2015; published 20 Feb 2015

17. G. D. Dice, S. Mujumdar, and A. Y. Elezzab, "Plasmonically enhanced diffusive and subdiffusive metal nanoparticle-dye random laser," Appl. Phys. Lett. **86**(13), 131105 (2005).
18. O. Popov, A. Zilbershtein, and D. Davidov, "Random lasing from dye-gold nanoparticles in polymer films: Enhanced at the surface-plasmon-resonance wavelength," Appl. Phys. Lett. **89**(19), 191116 (2006).
19. X. Meng, K. Fujita, Y. Zong, S. Murai, and K. Tanaka, "Random lasers with coherent feedback from highly transparent polymer films embedded with silver nanoparticles," Appl. Phys. Lett. **92**(20), 201112 (2008).
20. X. Meng, K. Fujita, S. Murai, and K. Tanaka, "Coherent random lasers in weakly scattering polymer films containing silver nanoparticles," Phys. Chem. A **79**(5), 053817 (2009).
21. Y. J. Lu, C. Y. Wang, J. Kim, H. Y. Chen, M. Y. Lu, Y. C. Chen, W. H. Chang, L. J. Chen, M. I. Stockman, C. K. Shih, and S. Gwo, "All-Color Plasmonic Nanolasers with Ultralow Thresholds: Autotuning Mechanism for Single-Mode Lasing," Nano Lett. **14**(8), 4381–4388 (2014).
22. Y. Wan, Z. Guo, X. Jiang, K. Fang, X. Lu, Y. Zhang, and N. Gu, "Quasi-spherical silver nanoparticles: Aqueous synthesis and size control by the seed-mediated Lee-Meisel method," J. Colloid Interface Sci. **394**, 263–268 (2013).
23. K. Aslan, Z. Leonenko, J. R. Lakowicz, and C. D. Geddes, "Annealed Silver-Island Films for Applications in Metal-Enhanced Fluorescence: Interpretation in Terms of Radiating Plasmons," J. Fluoresc. **15**(5), 643–654 (2005).
24. L. Ma, Z. Wu, and S. Ning, "Theoretical insight into the deep-blue amplified spontaneous emission of new organic semiconductor molecules," Org. Electron. **15**(11), 3144–3153 (2014).
25. M. A. Díaz-García, F. Hide, B. J. Schwartz, M. R. Andersson, Q. Pei, and A. J. Heeger, "Plastic lasers: semiconducting polymers as a new class of solid-state laser materials," Synth. Met. **84**(1-3), 455–462 (1997).
26. P. B. Johnson and R. W. Christy, "Optical Constants of the Noble Metals," Phys. Rev. B **6**(12), 4370–4379 (1972).
27. Y. Sivan, S. Xiao, U. K. Chettiar, A. V. Kildishev, and V. M. Shalaev, "Frequency-domain simulations of a negative-index material with embedded gain," Opt. Express **17**(26), 24060–24074 (2009).
28. X. Meng, K. Fujita, S. Murai, T. Matoba, and K. Tanaka, "Plasmonically controlled lasing resonance with metallic-dielectric core-shell nanoparticles," Nano Lett. **11**(3), 1374–1378 (2011).

1. Introduction

Recently, the metal nanoparticles (NPs) have been widely investigated for applications in various fields, and the interaction of metallic NPs and gain medium has attracted significant attention for photonic applications [1–9]. Metallic NPs exhibit the localized surface-plasmon resonance (LSPR), and the excitation of the plasmon absorption results in a strong local electromagnetic (EM) field enhancement in the vicinity of the Ag NPs. When they are excited by the light in resonance with their characteristic plasmon modes, metallic NPs can act as antennas at visible and near-infrared frequencies: they can modify the emission properties of optical emitters located near NPs, i.e., the Purcell effect [10–14].

Besides the modification of spontaneous emission properties, the stimulated emissions of emitters were also affected by metallic NPs. For example, the metallic NPs with periodic arrangement can act as a grating and lead to distributed feedback lasers [15, 16]; gold or silver NPs with random distribution were also found to lead to the random lasing by the effects of enhanced localized EM fields and scattering [17–20]. In addition, the metal nanostructures have been used as plasmonic nanocavities that rely on surface plasmons (SPs). Because the plasmon oscillations are coupled with gain media via the near field, the gain material localized in the vicinity of the metal surface could provide extra energy for the SPR loss compensation or amplification, and in return, the SPR mode provides a means of strength-related feedback for photons in the gain media. Thus, this laser can be called the surface plasmon amplification by stimulated emission of radiation (spaser) [7–9], which is nanoplasmonic counterpart of the laser. Although the spaser's theory and the plasmonic nanolasers were put forward and demonstrated, the more applications of the spaser are still desirable [4, 21].

In this letter, based on silver island films (SIFs), a very simple approach was demonstrated to tune lasing wavelength. SIFs with different size of silver NPs were used as the substrate, on which the gain media with planar waveguide structure were introduced. With the different LSPRs for SIFs, the lasing wavelengths were also determined by the corresponding LSPRs. The precisely tailored lasing was ascribed to the spaser by coupling between gain medium and plasmonic silver NPs.

#230988 - $15.00 USD Received 22 Dec 2014; revised 8 Feb 2015; accepted 8 Feb 2015; published 20 Feb 2015

2. Sample preparation and experimental setups

Ag NPs having a well-controlled size were synthesized by a seed-mediated growth method [22]. Different sizes of Ag NPs were prepared in two steps by citrate reduction of silver nitrate ($AgNO_3$) with $NaBH_4$ as strong reducing agent in water. First, small Ag NPs were synthesized under chemically reducing $AgNO_3$ in aqueous solution by a rapid nucleation-growth-ripening principle; the resulting Ag NPs were used as starter seeds. And then, we slowly added the proper portions of Ag salt and citrate reducer into the starter seeds solution as obtained in the first step. The slow process ensured aggregation of the released Ag atoms on the Ag nucleation centers without the formation of new centers. In this way, the final sizes of the NPs were tuned, and we prepared NPs with the diameters as: 8, 20, 50, 100, 200 and 500 nm.

SIFs were formed by the method of self-assembly. First, the clean glass substrate was soaked in the 1% aqueous solution of 3-aminopropyltriethoxysilane (APS) for 30 min at room temperature, then was washed extensively with deionized water and air-dried, and put it into Ag NPs aqueous solution for 12 h. Finally, the glass substrate with SIF was annealing at 120°C for 5 h to produce thermally stable SIFs. The annealing treatment can benefit to the fully evaporation of solvent and additive agent, keeping the good adhesion between SIF and glass substrate, and can also make the morphology of SIF more uniform [23]. Figure 1 shows the Atomic Force Microscopy (AFM) image and the corresponding size distribution of SIFs with different sizes.

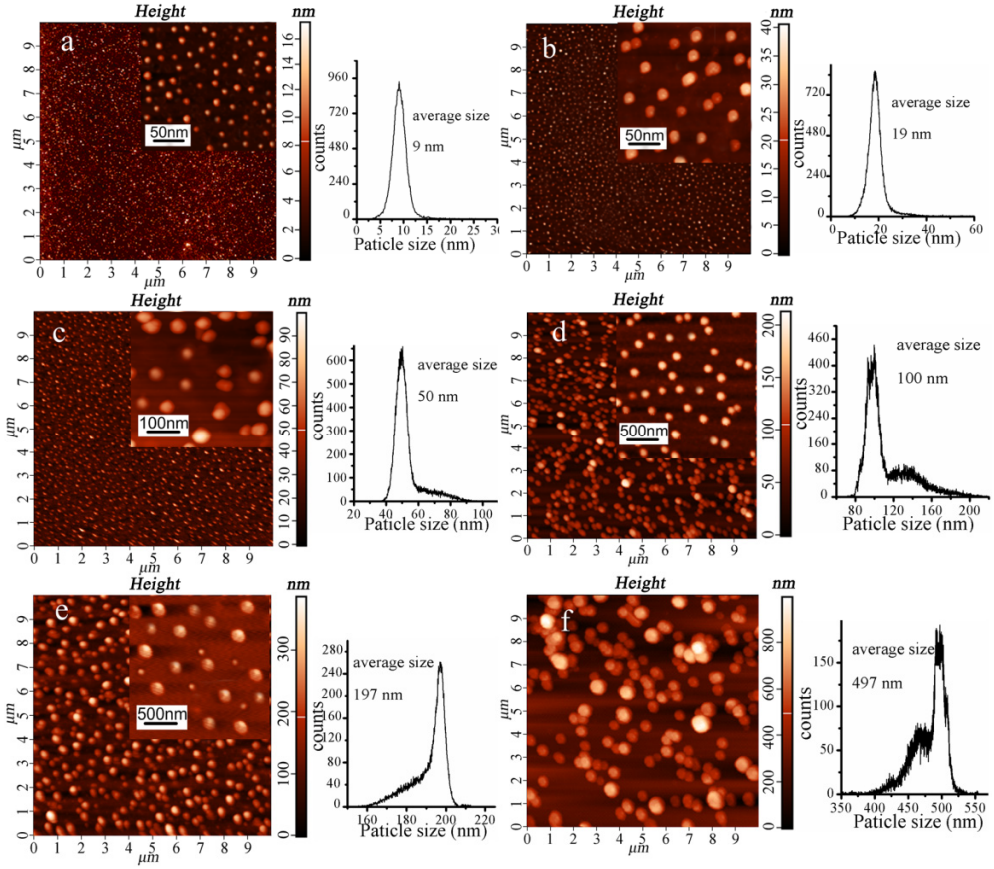

Fig. 1. AFM images of Ag NPs with different sizes prepared by self-assembly. The average sizes of Ag NPs are (a) 8 nm, (b) 20 nm, (c) 50 nm, (d) 100 nm, (e) 200 nm, and (f) 500 nm, respectively. The corresponding size distributions of particles are presented.

#230988 - $15.00 USD Received 22 Dec 2014; revised 8 Feb 2015; accepted 8 Feb 2015; published 20 Feb 2015

After the deposition of SIFs, the 5 nm-SiO_2 layer served as a spacer in order to avoid the quenching of the emission, was deposited onto the SIFs by radio frequency sputtering at the rate of 0.3 nm/s. N,N'-bis(3-methylphenyl)-N,N'-diphenyl- [1,1':4',1"-terphenyl] –4,4"-diamine (BMT-TPD) was used as gain medium [24]. The planar waveguide with gain medium was fabricated as follows: Polystyrene (PS) and BMT-TPD were fully dissolved in chloroform solution (PS: BMT-TPD = 4:1, wt%), and then was spin-coated on top of the SiO_2 layers with the speed of 4000 rpm, and the spin-coated films were annealed at 110 °C for 10 min. At last, the devices Glass/SIFs (8-500 nm)/SiO_2 (5 nm)/PS: BMT-TPD were fabricated. For comparison, the devices with 50 nm-thick SiO_2 spacer instead of that with 5 nm were prepared. And the device that gain medium was spin-coated onto glass substrate without any NPs was prepared. The thicknesses of organic gain media layer on SIFs with 8-200 nm Ag NPs are approximately 300 nm, and that of the gain media layer on SIFs with 500 nm Ag NPs is approximately 446 nm.

In experiments, the thickness of polymer film was measured with Stylus Profiler (Dektak 6M, USA). The absorption and photoluminescence (PL) spectra were obtained by UV-Vis spectrophotometer (HITACHI U-3010, Japan) and Fluorescence Spectrometer (fluoromax-4 spectrofluometer) respectively. The devices were pumped by the third harmonic of a Nd:YAG laser (355nm,10Hz repetition rate, and 25 ps pulse duration). Through a pinhole filter, a slit and a cylindrical lens, the laser beam was formed as a stripe with the size of 7 mm × 1 mm, and was perpendicular to the surface of the devices.

3. Results and discussion

The LSPR spectra of SIFs were measured. Figure 2 shows the LSPR spectra of SIFs with different sizes Ag NPs (without spacer layer), together with the emission spectrum of BMT-TPD. The peaks of LSPR are wavelengths of 388, 413, 424, 446, 464 and 488 nm, corresponding to the Ag NPs with the size of 8, 20, 50, 100, 200 and 500 nm shown in Table 1. It is clearly seen that the LSPR peaks of these different sizes of SIFs red-shift from 388 to 488 nm as the sizes of Ag NPs range from 8 nm to 500 nm. In the Fig. 2, it is also found that the LSPR spectra with the peak wavelength 413, 424, 446 and 464 nm for the 20-200 nm Ag NPs, sufficiently overlap with the emission spectrum of BMT-TPD, and as for the Ag NPs with 8 and 500 nm, the peaks of LSPR spectra are 388 and 488 nm, which are out of the scope of emission spectrum of BMT-TPD.

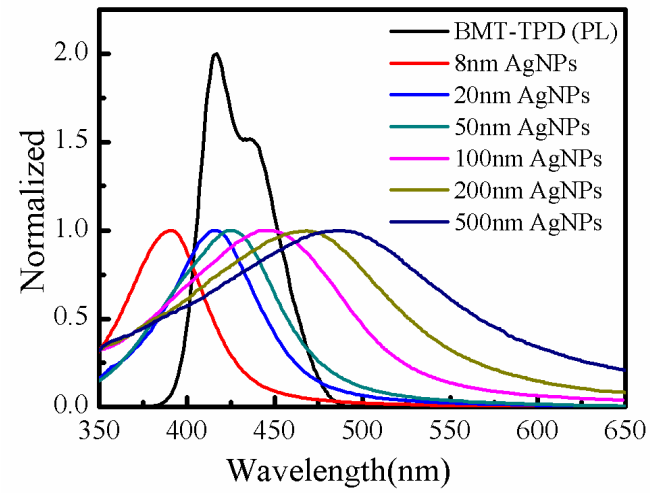

Fig. 2. The LSPR spectra of 8 nm Ag NPs (red line), 20 nm Ag NPs (blue line), 50 nm Ag NPs (green line), 100 nm Ag NPs (pink line), 200 nm Ag NPs (yellow line) and 500 nm Ag NPs (dark blue line), together with the emission spectrum of BMT-TPD (black line).

#230988 - $15.00 USD Received 22 Dec 2014; revised 8 Feb 2015; accepted 8 Feb 2015; published 20 Feb 2015

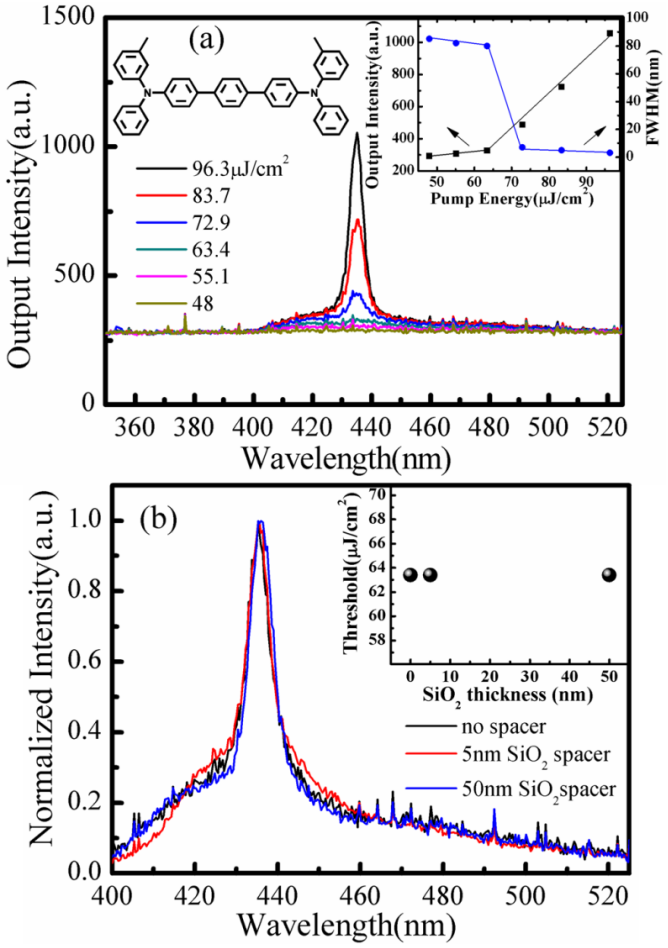

Fig. 3. (a) Dependence of edge-emission spectra of device glass/PS: BMT-TPD on the pump energy intensity. The inset shows the output intensity of the emission peak and FWHM as a function of pump energy for reference device without NPs. (b) The emission spectra of device glass/SiO_2 /PS: BMT-TPD pumped by 80 μJ /cm^2, in which the SiO_2 thicknesses are 0 nm (no spacer), 5 nm and 50 nm. The insert shows the lasing thresholds of the three devices.

In order to investigate the tailoring properties on the lasing wavelength, the devices Glass/SIFs (8-500 nm)/SiO_2 (5 nm)/PS: BMT-TPD were designed and discussed. Figure 4(a) shows the emission spectra of device based on the Ag NPs (8-500 nm) with 5 nm-SiO_2 spacer, together with a spectrum for the reference device without Ag NPs, which are all pumped by laser pulse of 60 μJ/cm^2. As mentioned in Fig. 3, the lasing threshold of reference device is 63.4 μJ/cm^2, so the reference device shows a broad emission spectrum centered at 435 nm under the excitation energy of 60 μJ/cm^2. However, the devices on SIFs with different size of Ag NPs have the lower lasing threshold. When they are pumped by the laser pulse of 60 μJ/cm^2, the lasing occurs and sharp peaks in the emission spectra appear, shown in Fig. 4(a). These lasing wavelengths are different when the gain medium of BMT-TPD on the different SIFs, that is, the lasing wavelength red-shifted from 416 nm to 466 nm with the increase of Ag NPs size from 8 to 500 nm. For comparison, we also prepared the devices with the 50 nm-thick spacer layer of SiO_2 instead of that of 5 nm. Figure 4(b) shows the emission spectra of these devices pumped by 80 μJ /cm^2. It is noticed that there is no obvious wavelength shift of lasing for the devices on different SIFs with 50 nm-thick spacer layer of SiO_2.

#230988 - $15.00 USD Received 22 Dec 2014; revised 8 Feb 2015; accepted 8 Feb 2015; published 20 Feb 2015

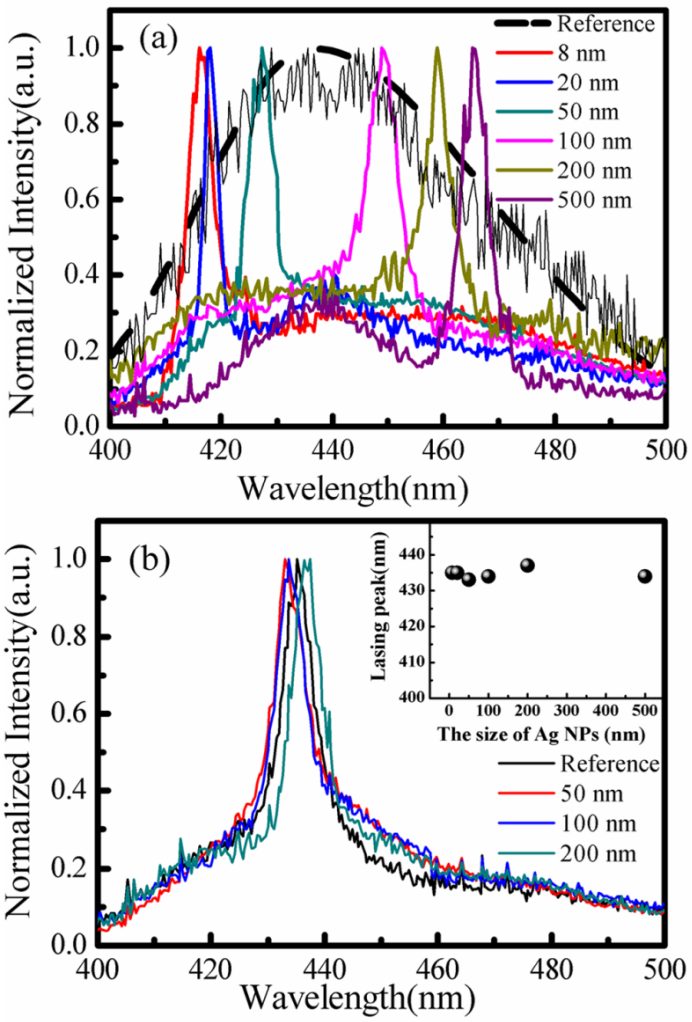

Fig. 4. (a) The emission spectra for devices based on SIFs (8-500 nm) with 5 nm- SiO_2 spacer, together with a spectrum for the reference device without Ag NPs, which are all pumped by laser pulse of 60 μJ/cm^2; (b) The emission spectra for devices based on SIFs (8-500 nm) with 50 nm-SiO_2 spacer pumped by 80 μJ/cm^2; The inset shows the lasing wavelength for the devices based on SIFs (8-500 nm) with 50 nm-SiO_2 spacer.

According to Fig. 2 and Fig. 4, the relation between the LSPR and the lasing wavelength can be summarized as the results in Fig. 5 and Table 1. As for the device with 5-nm-thick spacer layer, we found that when the LSPR peaks of Ag NPs are 414 nm, 426 nm, 446 nm and 466 nm, the corresponding lasing peaks are 418 nm, 427 nm, 448 nm and 459 nm, respectively, which shows that the lasing wavelength can be precisely tuned. When the LSPR peaks are 389 nm and 489 nm, the corresponding lasing peaks are 416nm and 466nm, respectively. As for the device with 50-nm-thick spacer layer, there is no systematic shift in the wavelength of lasing, and the lasing peak is always about 435 nm or so.

#230988 - $15.00 USD Received 22 Dec 2014; revised 8 Feb 2015; accepted 8 Feb 2015; published 20 Feb 2015

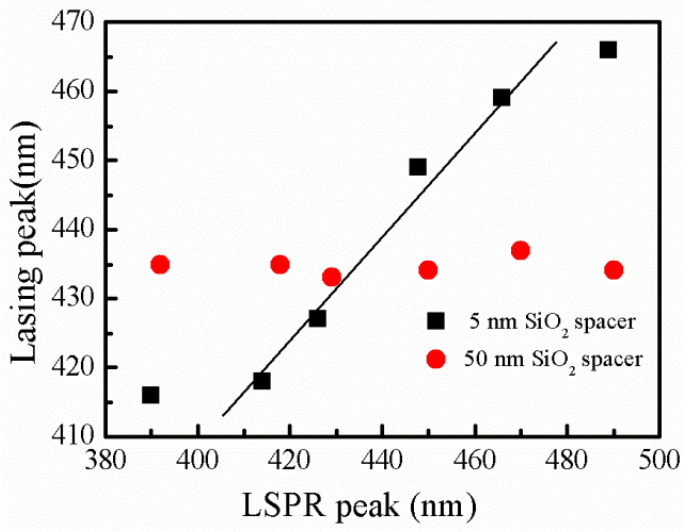

Fig. 5. The relation between the wavelength of the lasing and that of the LSPR. Solid blocks correspond to the devices based on SIFs with 5 nm-SiO_2 spacer, solid circles correspond to the device based on SIFs with 50 nm-SiO_2 spacer.

Table 1. The relation between the LSPR of Ag NPs and the lasing wavelength. D is the diameter of Ag NPs. W_{LSPR} is the wavelength of LSPR peak for the SIFs without spacer layer. $W_{LSPR\text{-}5nm}$ ($W_{LSPR\text{-}50nm}$) is the wavelength of LSPR peak for the SIFs deposited with 5 nm (50 nm) SiO_2 spacer layer. $W_{Lasing\text{-}5nm}$ ($W_{Lasing\text{-}50nm}$) is used to represent the lasing wavelength of dyes based on the Ag NPs (8-500 nm) with 5 nm (50 nm) SiO_2 spacer.

D (nm)	W_{LSPR} (nm)	$W_{LSPR\text{-}5nm}$ (nm)	$W_{Lasing\text{-}5nm}$ (nm)	$W_{LSPR\text{-}50\ nm}$ (nm)	$W_{Lasing\text{-}50nm}$ (nm)
	no spacer	5 nm spacer		50 nm spacer	
8	388	389	416	391	435
20	413	414	418	416	435
50	424	426	427	428	433
100	446	446	448	448	434
200	464	466	459	469	437
500	488	489	466	490	434

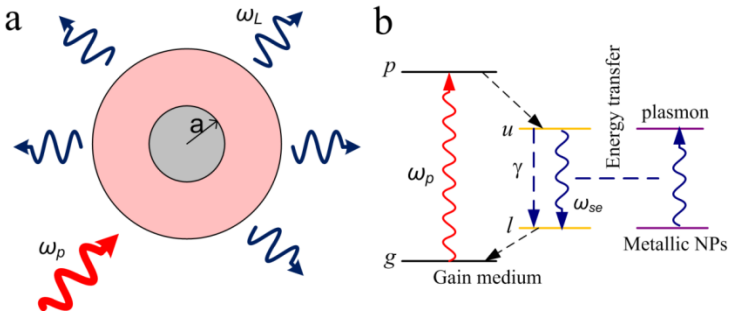

Fig. 6. (a) the metallic particle of radius *a* located in the gain medium. (b) Straight lines denote the transition rates, and wavy lines denote the frequencies of the transitions.

Based on the observation that lasing frequency is near LSPR frequency, the spaser theory is put forward to explain our experiment results. In our device, the Ag NPs were used as the plasmonic nanocavities and organic laser dyes was used as optical gain media to compensate the plasmon losses. Figure 6(a) shows the metallic particle of radius *a* located in the gain medium. The gain media is pumped by an electromagnetic wave of frequency ω_p, exciting the dye molecules from ground state *g* to pumped state *p*, see Fig. 6(b). Laser transition occurs

#230988 - $15.00 USD Received 22 Dec 2014; revised 8 Feb 2015; accepted 8 Feb 2015; published 20 Feb 2015

between upper and lower laser states u and l, respectively, and the frequency of the spontaneous emission is ω_{se}. However, in the spaser geometry, the photoemission is strongly quenched due to the resonance energy transfer to the SP modes. The plasmons in the spaser mode create the high local fields that excite the gain medium and stimulate more emission to this mode, which is the feedback mechanism.

According to the papers for the spaser [7, 8], we can get the spasing frequency as follow:

$$\omega_L = \frac{\omega_{sp}/\Gamma_{sp} + \omega_{se}/\Gamma}{1/\Gamma_{sp} + 1/\Gamma} \tag{1}$$

which implies that the lasing frequency ω_L lies between the extinction maxima (SP frequency) ω_{sp} and the spontaneous emission frequency of the gain medium ω_{se}. As for the data of Table 1 in our paper, the lasing wavelength is also in according with Eq. (1). For detail, as for the 20, 50, 100 and 200 nm Ag NPs, the corresponding LSPR responses are 414, 426, 446 and 466 nm, respectively. Those LSPR peaks are located near or in the range of full width at half maximum (FWHM) of spontaneous emission spectrum of the gain medium shown as Fig. 2. The extinction maxima of SP could enhance photonic density of states at corresponding wavelength of gain medium. So that we can consider the spontaneous emission frequency of the gain medium ω_{se} is equal to the corresponding SP frequency ω_{sp} of Ag NPs. According to the Eq. (1), when the $\omega_{se} \approx \omega_{sp}$, the spaser frequency ω_L is equal to the extinction maxima (SP frequency) ω_{sp}. However, as for the Ag NPs with size of 8 nm and 500 nm, the corresponding LSPR response are 389 and 489 nm, which are deviating from the scope of spontaneous emission spectrum too much, and the $\omega_{se} \neq \omega_{sp}$. Therefore, the spaser frequency ω_L lies between the extinction maxima (SP frequency) ω_{sp} and the spontaneous emission frequency of the active medium ω_{se}. The data of Table 1 is in agreement with description of Eq. (1).

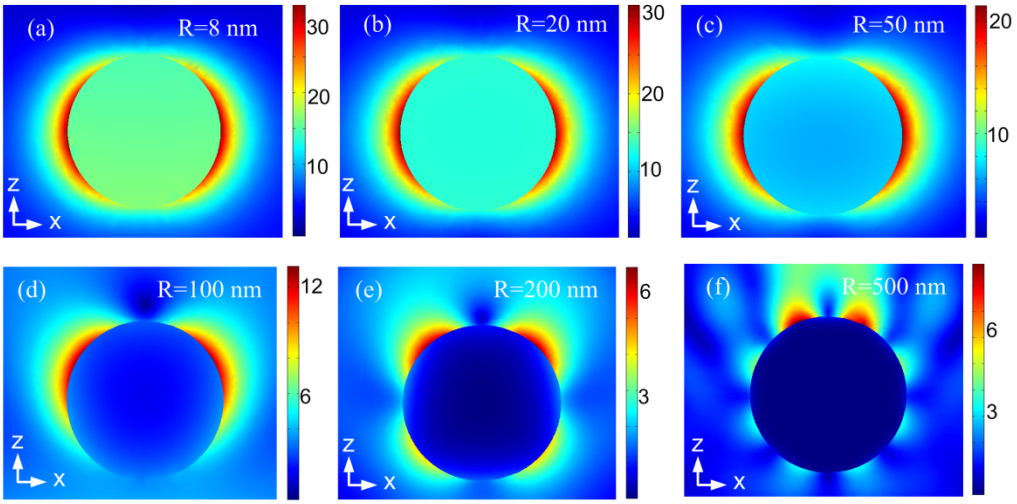

Fig. 7. The electric-field distribution of the (a) 8 nm, (b) 20 nm, (c) 50 nm, (d) 100 nm, (e) 200 nm and (f) 500 nm Ag NPs surrounding by the gain medium, which were calculated under the excitation at their plasmon wavelengths.

#230988 - $15.00 USD Received 22 Dec 2014; revised 8 Feb 2015; accepted 8 Feb 2015; published 20 Feb 2015

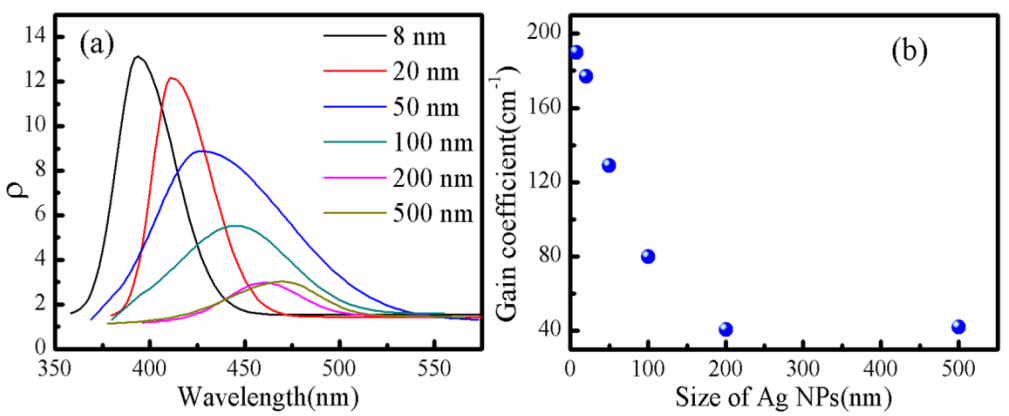

Fig. 8. (a) Average electric-field enhancement, (b) The gain coefficient, for the gain medium with different size of Ag NPs.

In order to more precisely explained our experimental results, the simulations of local fields around the nanoparticles with different size located in the gain medium were performed using the finite element method based on the commercial software COMSOL. In these simulations, the complex permittivity values of silver are from [26], and the complex refractive index of gain medium is measured by the Ellipsometer. Figure 7 shows the electric-field distribution of the different size of Ag NPs surrounding by the gain medium, which were calculated under the excitation at their plasmon wavelengths. According to the reference [27], the average electric-field enhancement is as follow:

$$\rho = \sqrt{\int |E(\vec{x},\lambda)|^2 \, d^3x \Big/ \int |E_{inc}|^2 \, d^3x} \qquad (2)$$

Figure 8(a) shows the average electric-field enhancement for all the devices with different size of Ag NPs. It knows the effective gain is determined by the average electric-field enhancement [27]. According to the simulation result of average electric-field enhancement, we can also find that for the different size of Ag NPs, there are strongest enhanced fields near their plasmon wavelengths. For gain medium with different size of Ag NPs, the average field enhancement amounts to an increase of the gain coefficient g (g = 14.5 cm^{-1}) by a factor of up to $|E/E_{inc}| \approx \rho_{max}^2$, ρ_{max} is the electric-field enhancement at the plasmon wavelengths shown in Fig. 8(a), so that the gain coefficient $g_{eff} \approx \rho_{max}^2 g$. According to the Eq. (2) and Fig. 8(a), giving the ρ_{max} of 13.1, 12.2, 8.9, 5.5, 2.8 and 2.9 for the Ag NPs with 8, 20, 50, 100, 200 and 500nm, respectively. The corresponding gain coefficient g_{eff} can be calculated and shown in Fig. 8(b).

As for the device with 5-nm-thick spacer layer, the tunable lasing is due to the spaser from the interaction between plasmonic Ag NPs and gain medium. As we know in the previous reports [28], the effect of LSPR is confined in the local area, and the scope of LSPR effects is in 40 nm or so. For example, in Meng' s report [28], by the simulation of spatial distribution of electric field intensity for the Ag NPs, they used 34-nm-thick SiO_2 shell to encapsulate Ag NPs, which avoided the LSPR effect on the organic lasing dyes near to these Ag NPs. So, the role of 5 nm-thick spacer is used to avoid the quenching effect of the dyes near to the metal, while the LSPR effect of Ag NPs is still on. However, when thickness of the spacer layer is increased to 50 nm, the LSPR effect of Ag NPs is avoided fully, and there is no coupling between the LSPR and the dye molecules. Without the assistance of LSPR effect, the spaser was avoided, and the emission spectrum was from the ASE of gain medium, and the wavelength of lasing was almost kept, shown in Fig. 4 (b) and Fig. 5.

#230988 - $15.00 USD Received 22 Dec 2014; revised 8 Feb 2015; accepted 8 Feb 2015; published 20 Feb 2015

4. Conclusion

In summary, we demonstrated an easy approach for tuning the lasing of BMT-TPD using the different SIFs. These SIFs have the different size of Ag NPs ranged from 8 to 500 nm, which exhibited the different LSPR spectra. We demonstrated the wavelength tuning of the lasing on the different SIFs. These behaviors were attributed to the spaser from the coupling between gain medium and LSPR of silver NPs, which resulted in the lasing at the corresponding wavelengths.

Acknowledgements

This work was financially supported by Basic Research Program of China (2013CB328705), National Natural Science Foundation of China (Grant Nos. 61275034), Ph.D. Programs Foundation of Ministry of Education of China (Grant No. 20130201110065).

#230988 - $15.00 USD Received 22 Dec 2014; revised 8 Feb 2015; accepted 8 Feb 2015; published 20 Feb 2015